Modulation of the Silica Sol-gel Composition for the Promotion of Direct Electron Transfer to Encapsulated Cytochrome c
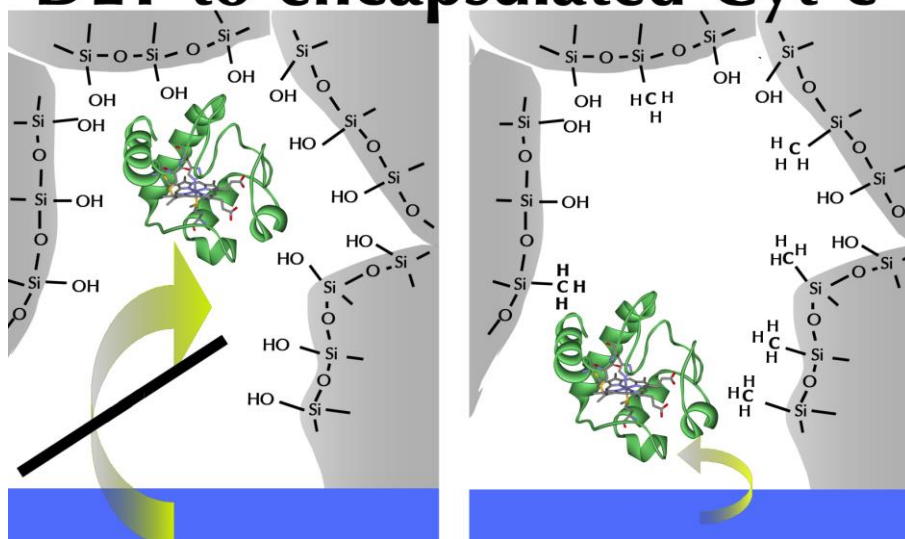
Alonso Gamero-Quijano[1], Francisco Huerta[2], Emilia Morallón[1], Francisco Montilla[1]

[1]Dept. Química Física e Instituto Universitario de Materiales, Universidad de Alicante, Ap. 99, E-03080, Alicante, Spain

[2]Dept. Ingeniería Textil y Papelera, Universitat Politècnica de Valencia, Plaza Ferrandiz y Carbonell, 1. E-03801, Alcoy, Spain

Graphical abstract

Abstract

The direct electron transfer between indium-tin oxide electrodes (ITO) and cytochrome c encapsulated in different sol-gel silica networks was studied. Cyt c@silica modified electrodes were synthesized by a two-step encapsulation method mixing a phosphate buffer solution with dissolved cytochrome c and a silica sol prepared by the alcohol free sol-gel route. These modified electrodes were characterized by cyclic voltammetry, UV-visible spectroscopy and in situ UV-visible spectroelectrochemistry. The electrochemical response of encapsulated protein is influenced by the terminal groups of the silica pores. Cyt c does not present electrochemical response in conventional silica (hydroxyl terminated) or phenyl terminated silica. Direct electron transfer to encapsulated cytochrome c and ITO electrodes only takes place when the protein is encapsulated in methyl modified silica networks.

Keywords

1. Introduction

The direct electron transfer from conducting materials to biomolecules, particularly proteins, has become a central issue in the development of certain biotechnological devices such as biofuel cells or chemical biosensors [1-3]. Bioelectrochemical studies on proteins have reported useful information about the structural organization of these molecules in contact with surfaces, the electron transfer characteristics to electrodes or the electron transfer processes in biological systems [2,4-7].

Enzymes, as specific protein catalysts, have been used for the detection of a number of analytes, triggering the development of electrochemical biosensors and becoming a trending topic in electroanalysis during the last few years. Usual amperometric biosensors make use of redox mediators which are immobilized on the electrode surface. These mediators, usually ferrocene species, have the ability of carrying electrons from the enzyme molecule to the electrode [8-10]. However, current scientific attention focuses on the development of the so-called third generation of biosensors. In such devices, the direct electron transfer take place between enzyme molecules and electrode surfaces with no redox mediation [11-14].

For the development of these applications, direct electron transfer to immobilized proteins is preferable because it delivers better electrochemical responses. Accordingly, several strategies for the immobilization of enzymes have been assayed: covalent binding [15,16], physical adsorption [17-21] or encapsulation within polymeric matrices [22]. Promising results have been obtained for enzyme encapsulation in inorganic matrices such as silica synthesized by sol-gel processes [9,23-25]. Encapsulation within silica networks provides soft immobilization conditions that prevent denaturalization of biomolecules upon encapsulation [26,27]. In addition, the silica structure offers protection

4

against some bulk solution components, thus reducing the risk of denaturation because of pH or ionic strength effects [28].

The electrostatic interactions between silica materials and encapsulated biomolecules are very relevant in the optimization of these systems for bioelectrochemical applications [29,30]. Specifically, it is known that silica pores may be tailored to favor certain enzyme orientations which allow the substrates reaching their active sites easily. A key aspect in pore modification is the tuning of their polarity, which can be achieved by copolymerization of suitable organosilane precursors with the usual tetralkoxide silica precursor. The resulting organic-inorganic hybrid material is known as *ormosil*, i.e. an *organic-modified silica*. These hybrid materials show different affinity for polar structures thereby modulating the stability and functionality of the encapsulated biomolecules [24,27].

In the present work we have examined the viability of inducing direct electron transfer between electrode surfaces and biomolecules encapsulated in silica materials. The selected model molecule was the redox active protein cytochrome c (cyt c). Cyt c is a water soluble hemoprotein acting as electron transducer during the biological respiratory chain thanks to its capability to undergo redox transformations [31]. Several bioelectrochemical devices take advantage of this redox ability, for example cyt c has been used as electron acceptor in the cathode of glucose-oxygen biofuel cells [1,32]. It has been also demonstrated that the electrical current in microbial fuel cells is wired to the electrode through this type of proteins, which are present in the membrane of *Geobacter sulfurreducens* bacteria. Walcarius et al. have shown in a recent report the physical entrapment of bacteria (*Pseudomonas fluorescens*) in a porous sol–gel matrix deposited as a thin layer onto an electrode along with cytochrome c [33]. The protein acts as redox

mediator providing an effective way to develop an 'artificial' biofilm that mimics the charge transfer processes of natural biofilms.

Our goal is to develop a suitable method for the encapsulation of cyt c in different silica sol-gel materials (based on both inorganic and hybrid networks). A detailed electrochemical study of the electrode modified with encapsulated cyt c will be performed. Finally, the influence of the protein structural state on its electrochemical behavior and the effect of the silica matrix composition on the electrochemistry of the encapsulated biomolecule will also be investigated.

2. Experimental part

2.1. Reagents and equipment

Tetraethyl orthosilicate (TEOS) were purchased from Sigma-Aldrich, hydrochloric acid (Merck, p.a.), triethoxy(methyl)silane (MTES) Sigma-Aldrich, triethoxy(phenyl)silane PhTES Sigma-Aldrich, cytochrome c (cyt c) from horse-heart 98% Sigma-Aldrich, Potassium dihyhydrogen phosphate (Merck, p.a.), Di-potassium hydrogen phosphate (Merck, p.a.), all the solutions were prepared with ultrapure water obtained from an Elga Labwater Purelab system (18.2 MΩ cm). The electrochemical cells were purged by bubbling a N$_2$ flow for 20 min, and the N$_2$ atmosphere was maintained during all the experiments. The counter electrode was a platinum wire. All potentials were measured against a reversible hydrogen electrode (RHE). Indium-tin oxide (ITO) covered glass substrates (Delta, CG-60IN, 60 S cm^{-1}) were used as working electrodes. Prior to its use, the ITO glass was degreased by sonication in an acetone bath and rinsed with an excess of deionized water, then an etching treatment was carry out with 37% w/w HCl to

define a working geometric area of $1cm^2$ for each ITO electrode. Cyclic voltammograms were performed with a potentiostat (eDAQ EA161) and a digital recorder (eDAQ, ED401) with eDAQ EChart data acquisition software. UV-vis spectra were acquired with a JASCO V-670 spectrophotometer using quartz cells with 1cm of optical path. *In-situ* UV-vis spectra were performed using an ALS model SEC-C05 Thin Layer Quartz Glass Spectroelectrochemical cell. The wettability (contact angle) of silica materials were measured with a Ramé-Hart 100 (Ramé-hart, inc, Mountain Lakes, NJ, USA) instrument at 25°C.

2.2 Preparation of electrodes

Two stock solutions were prepared as follows:

Solution 1, silica precursor solution, prepared by mixing 2.00 mL of TEOS (8.96 mmol) with 1.26mL of HCl 0.01M under vigorous stirring at room temperature in a closed vessel. After 2 hours, the resulting sol was submitted to rota-evaporation until the complete removal of the stoichiometric amount of ethanol released from the hydrolysis reaction [34]. Alternatively, organic-modified silica (*ormosil*) was prepared following a similar procedure, but replacing part of the TEOS precursor by an organic triethoxysilane precursor (PhTES or MTES). The total moles of silica precursor were kept constant (8.96 mmol). The resulting *ormosil* network is labeled as $SiO_{(2-0.5x)}R_x$ where x represent the mole fraction of the organic moieties in the resulting solid gel.

Solution 2, cytochrome c solution (1 mg/mL) was prepared by dissolving the protein in a phosphate buffer solution (PBS, pH 7) made of K_2HPO_4 0.15M + KH_2PO_4 0.1M.

For the encapsulation and immobilization of cytochrome c on the electrode 40µL of solution 1 were placed in an Eppendorf vial and mixed with 40µL of solution 2. The concentration of the protein in this solution was 40 µM. This mixture was dispensed over a clean ITO electrode. After a time period of 20-40 s a homogeneous silica gel is formed over the ITO surface.

3. Results and discussion

3.1. Characterization of cyt c in solution

UV-visible spectroscopy has been used to get information on the structural state of dissolved cytochrome c at different pH values. Fig. 1 shows the UV-visible spectra of cytochrome c in either PBS or 0.5M H_2SO_4 electrolyte solutions.
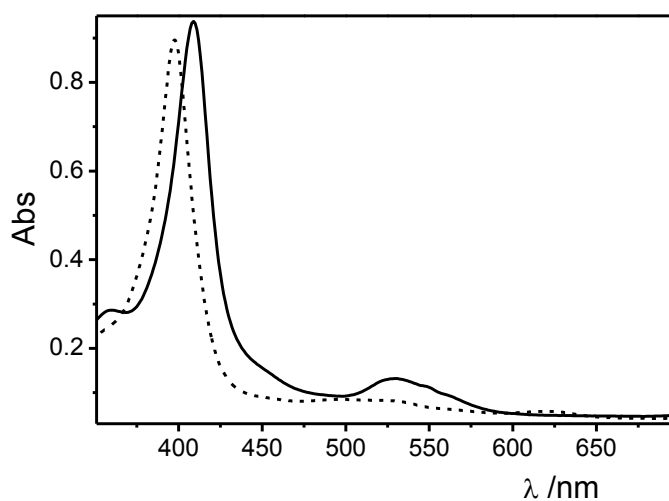

Figure 1. UV-visible spectra recorded for cytochrome c in PBS (pH=7, solid line) and in 0.5M H_2SO_4 (dashed line) solutions.

Under neutral pH conditions, cytochrome c is in its native state and two characteristic bands can be observed in the electronic spectrum. On the one hand, the so-called Soret band at 409 nm and, on the other, a broad band centered at around 535nm. This latter feature holds the contribution from the poorly defined α and β absorption bands of the heme group[32,35].

The UV-visible spectrum of cyt c in strong acidic conditions shows a blue-shifted Soret band peaking at 398 nm and an almost undetectable couple of α and β bands. The latter spectrum is characteristic of the denaturalized state of cyt c.

The electrochemical characterization of cyt c in aqueous solution was carried out by cyclic voltammetry. Fig. 2.a shows the steady-state cyclic voltammogram recorded for an ITO electrode immersed in a solution containing 0.5 mg/mL cyt c in phosphate buffer.
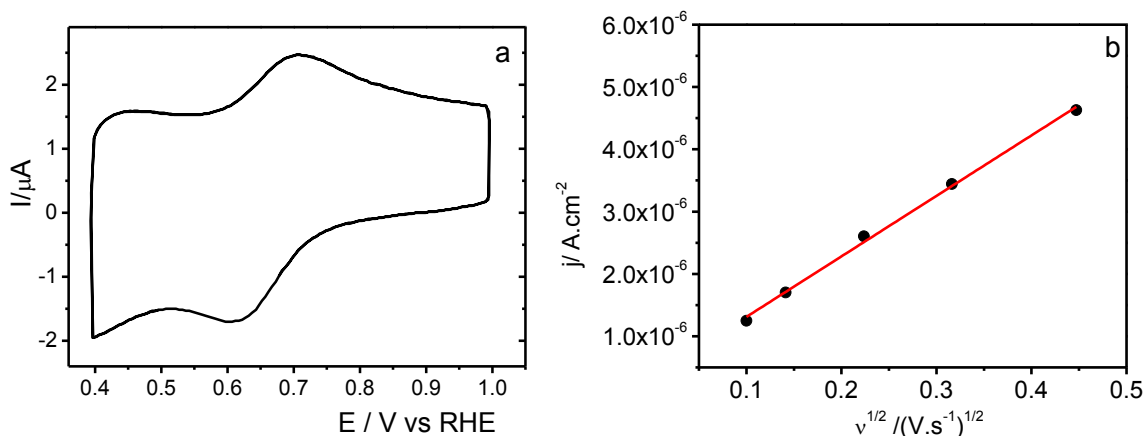
Figure 2. (a) Steady-state cyclic voltammogram of an ITO electrode in a 0.5 mg/mL cyt c in PBS. Scan rate: 100mV/s; **(b)** Randles-Sevcik plot of anodic peak current *vs* the square root of the scan rate.

During the forward potential scan, a broad anodic peak appears centered at 0.71V. This feature is linked with the oxidation of the ferrocytochrome c to form ferricytochrome c. During the reverse scan, the cathodic peak centered at 0.61V reveals the reduction of ferricytochrome c. The formal potential for cyt c redox transition can be evaluated from the mean of the peak potentials, $E^{o\prime} = \frac{E_{pa}+E_{pc}}{2} = 0.66$V vs RHE (0.25V vs NHE). This value is in good agreement with literature data [36-40]. From ΔE_p we have determined the value of the standard heterogeneous rate constant for the electron transfer, k^o, which amounts to 6.60×10^{-4} cm s^{-1}. The details of the calculations are given elsewhere [41]. The obtained k^o value is also consistent with bibliographic data reported for graphite and ITO electrodes[37,39].

Cyclic voltammograms were carried out at different scan rates and the plot of anodic peak currents vs the square root of scan rates shows a linear trend, as can be observed in Fig. 2.b. From the Randles-Sevcik equation, a value of 4.7×10^{-7} cm^2 s^{-1} for the diffusion coefficient of cytochrome c in solution was calculated, in good agreement with the literature data [37,39,42]. These voltammetric experiments were conducted in PBS solution, were the cytochrome c molecule remains in its native state. Cyclic voltammetry studies performed in strongly acidic conditions (0.5M H$_2$SO$_4$) resulted in no electrochemical response for the dissolved protein, indicating that the protein in denaturalized state shows no redox activity in solution at ITO electrodes.

The evolution of the spectral features upon electrochemical reduction was studied by *in situ* electrochemical UV-vis spectroscopy in a solution containing cyt c in PBS medium and the results are presented in Fig. 3. The experiment was initiated by acquiring one spectrum under open-circuit conditions (dotted lines) and then a reduction potential of +0.2 V was applied. Additional spectra were subsequently acquired every 600 s to gain information about the effect of the applied potential on the UV-visible spectrum. Initially, the Soret band at 409 nm together with the couple of overlapped α and β-bands in the vicinity of 535 nm can be clearly observed. Both the frequency and the intensity of these features are typical of the oxidized state of cytochrome c [32,35].
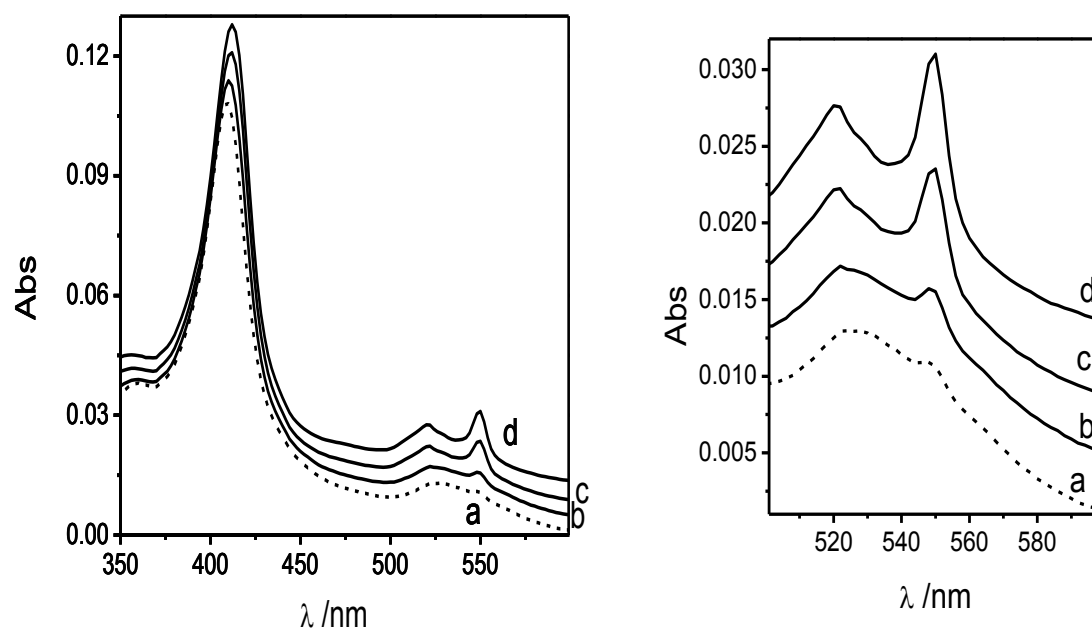
Figure 3. *In situ* UV-visible spectra of cytochrome c (0.2mg/mL) in PBS at open circuit (a) and after the application of a reduction potential of +0.2 V vs RHE for: 600 s (b), 1200 s (c) and 1800 s (d).

When the potential is stepped to +0.2 V vs RHE the spectrum undergoes slight but significant modifications due to the reduction of cyt c. The Soret band shifts 3 nm to red and its intensity increases upon electrochemical reduction. More important changes are observed for α and β bands. The intensity of both features increases progressively during the reduction treatment and, simultaneously, they become resolved after 1800 s. The α-band peaks at 549 nm and the β-band at 520 nm at the end of the experiment.

3.2. Characterization of encapsulated cyt c in silica

Fig. 4.a shows the cyclic voltammogram of cyt c@SiO$_2$ modified electrode immersed in a PBS solution. This voltammogram exhibits the characteristic double layer of an ITO electrode with no redox process related with cytochrome activity.
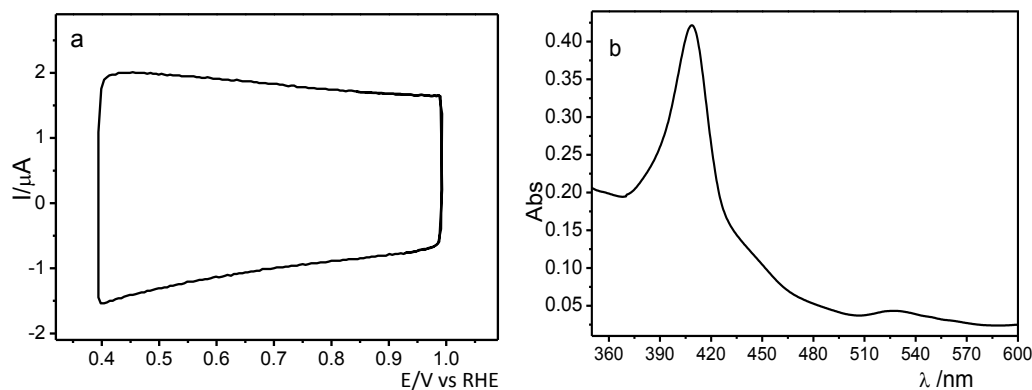

Figure 4. (a) Steady-state cyclic voltammogram recorded in PBS medium for a cyt c@SiO$_2$ modified electrode. Scan rate: 100mV/s; **(b)** UV-Vis spectrum acquired for a ITO-cyt c@SiO$_2$ immersed in PBS solution.

The UV-visible spectrum in Fig. 4.b was recorded to check both the presence of encapsulated cytochrome and its structural state. The spectrum shows the two characteristic set of features: a Soret band at 409 nm and overlapped bands at around 535 nm. The frequency of both features reveals that cyt c is encapsulated in its native form, while the lack of band resolution at around 535 nm indicates that the biomolecule is in the oxidized state. This result points that cyt c, like other hemoproteins, retains its characteristic optical signatures upon sol-gel encapsulation[25,43-47]. In addition to the *ex*

situ spectrum of Fig. 4.b, *in situ* spectroelectrochemical experiments were also carried out to follow the possible electrochemical reduction of encapsulated cyt c through the evolution of the corresponding absorption bands. However, no spectral modifications can be observed in such experiment (see Fig. S1 in the Supporting Information), which confirms the lack of electron transfer between the ITO electrode and the encapsulated molecule.

The lack of charge transfer may be ascribed to the electrostatic interactions appearing between cyt c and the surface of the silica pores. It is known that the isoelectric point of cyt c is around 10, so this molecule is positively charged at the neutral pH of the experiments [48]. On the contrary, silica presents an isoelectric point in the range of 1.7-3.5 and, therefore, it is negatively charged in the PBS electrolyte used here [49,50]. The opposite charges cause an electrostatic interaction of cyt c and silica walls which probably prevents the protein to reach more favorable orientation for the electron transfer, as suggested by Keeling-Tucker et al. [29,51].

It is known that ormosils can provide silica structures with different degrees of hydrophobicity and the associated change in the pore polarity may favor the electron transfer with the electrode [52-54]. So, at this point, the chemical modification of the silica is studied in order to obtain structures able to modulate the electrostatic interactions between the silica walls and cyt c.

Fig. 5 shows cyclic voltammograms and UV-vis spectra for cyt c encapsulated within two different ormosil-modified electrodes: phenyl-modified silica (solid line) and methyl-modified silica (dashed line). The chemical formula $SiO_{(2-0.5x)}R_x$, where R can be either Ph or Me group, has been used to describe the expected degree of substitution

in the chemical structure of the resulting material. The amount of organic groups was
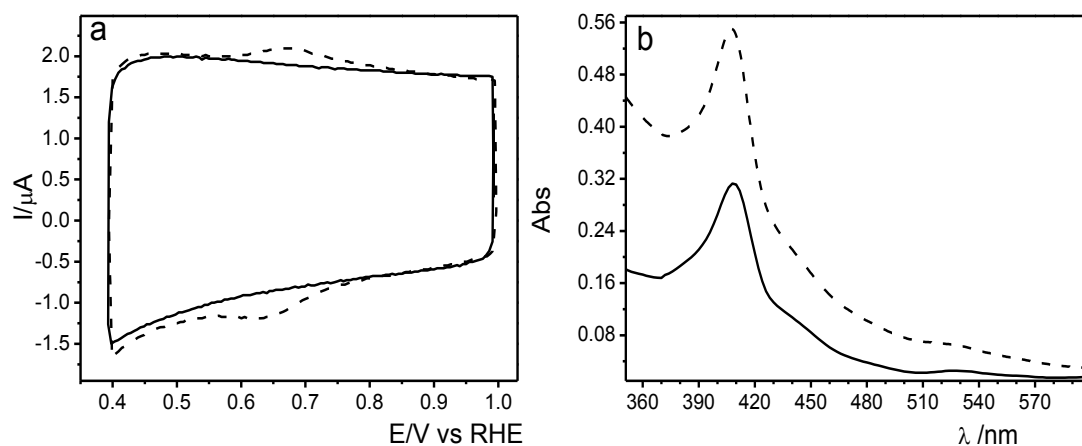
set at $x=0.1$ for the experiments shown in Fig. 5.

Figure 5. (a) Steady-state cyclic voltammograms of cyt c@$SiO_{1.95}Ph_{0.1}$ (solid line) and

cyt c@$SiO_{1.95}Me_{0.1}$ (dashed line) modified electrodes in PBS. Scan rate: 100mV/s; **(b)**

UV-Vis spectra of Cyt C@$SiO_{1.95}Ph_{0.1}$ (solid line) and cyt c@$SiO_{1.95}Me_{0.1}$ (dashed line)

immersed in PBS.

The cyclic voltammogram for cyt c@$SiO_{1.95}Ph_{0.1}$ of Fig.5.a shows only the

characteristic double layer charging of the supporting electrode. Cyt c offers no

electrochemical response from the inside of the phenyl-modified *ormosil*. Phenyl

moieties introduce hydrophobic terminal groups in the silica gel which decrease the

pore polarity. The corresponding increase in hydrophobicity of the resulting *ormosil*

was assessed by contact angle measurement (see Table S1 in Supporting Information).

Although phenyl-modified silica is more hydrophobic than pure SiO_2, no

electrochemical response is obtained after the inclusion of these groups. Furthermore, the introduction of higher amounts of phenyl groups (up to $x= 0.32$) does not modify the obtained result.

The lack of electrochemical response could have been attributed to the denaturalization of the encapsulated protein. However, the UV-visible spectrum displayed in Fig. 5.b shows that the characteristic cyt c electronic absorptions are retained and, accordingly, that the biomolecule is in its oxidized and native state. Additional *in situ* electrochemical UV-vis studies were carried out to confirm that no direct electron transfer takes place under the experimental conditions employed. A reduction potential of 0.2V was applied during 2000 s to the phenyl modified silica containing the encapsulated biomolecule (see Fig. S2 in the Supporting Information). Since no changes in the UV-vis spectra are observed, it is deduced that the immobilized cyt c does not undergo any change in its oxidation state, in agreement with the absence of redox response observed in the voltammogram of Fig 5.a.

Fig. 5 also shows the electrochemical and the spectroscopic characterization of cyt c encapsulated in a silica gel containing methyl groups ($SiO_{1.95}Me_{0.1}$). Methyl-modified silicas present higher hydrophobicity than the corresponding phenyl derivatives, as deduced from the contact angle measurements (see Table S1 in the Supporting Information). The dashed line in the cyclic voltammogram of Fig.5.a shows a pair of peaks (oxidation at 0.68V and reduction at 0.63V) clearly related with a redox process at the cytochrome heme center.

The intensity of this electrochemical response of the encapsulated protein depends strongly on the amount of methyl groups in the silica network. Figure 6 shows cyclic

voltammograms recorded for different cyt c@SiO$_{(2-0.5x)}$Me$_x$ modified electrodes, where the mole fraction of methyl groups was varied from 0.1 to 0.42.
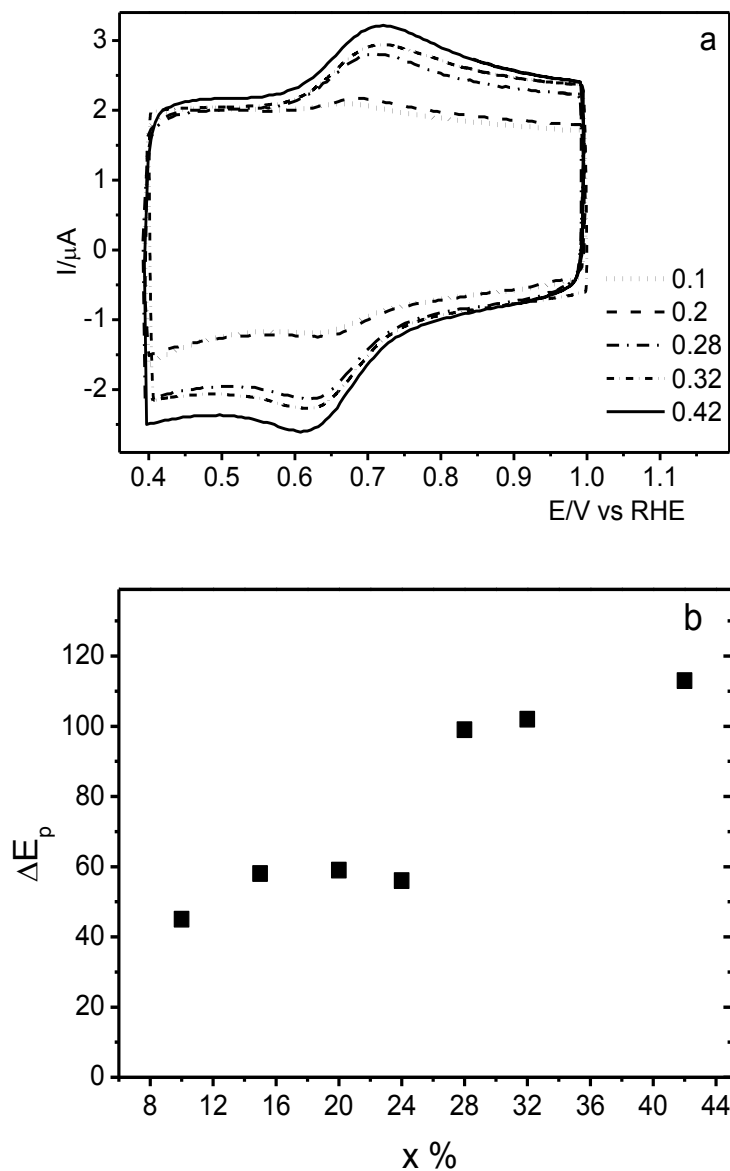

Figure 6. (A) Cyclic voltammograms for cyt c@SiO$_{(2-0.5x)}$Me$_x$ modified electrodes in PBS. The mole fraction of methyl goups (*x*) is indicated for each line. Scan rate: 100mV/s. (B) Voltammetric peak separation for encapsulated cyt c redox process as a function of the methyl mole fraction in the *ormosil* structure.

The electrochemical studies have been limited to methyl mole fractions below $x=0.42$ because the mechanical stability of the silica film is poor beyond that value. This effect is probably due to the lower cross-linking induced by the excess of methyl groups in the final material [29].

These voltammetric curves show that the cytochrome redox process is barely detected for methyl-modified electrodes with x lower than 0.2, but well-defined features can be observed for higher methyl amounts. Since the encapsulated cyt c formal potential derived from these curves keeps constant at 0.66 V, it can be assumed that the inclusion of methyl groups inside the silica network does not induce conformational changes in the cytochrome structure. This assumption will be confirmed later by UV-vis spectroscopy.

From the CVs in Fig. 6a it is possible to follow the evolution of the peak separation for the iron redox process, ΔE_p, with the mole fraction of methyl groups present in the silica gel. The results obtained are shown in Fig. 6b, where it is observed that mole fractions below 0.28 lead to low peak separations of about 40-60 mV. Such figures strongly suggest that the redox process is electrochemically reversible at moderate methyl substitution. However, a sudden increase of the peak separation is observed for mole fractions above 0.28. Indeed, cytochrome immobilized in highly methylated silica materials shows ΔE_p around 100 mV, a value which is characteristic of quasi-reversible electrochemical processes.

In order to gain more insight into the nature of the electron transfer process, cyclic voltammetry experiments for cyt c encapsulated in a set of methyl-modified silica were performed at different scan rates (see Fig. 7a).
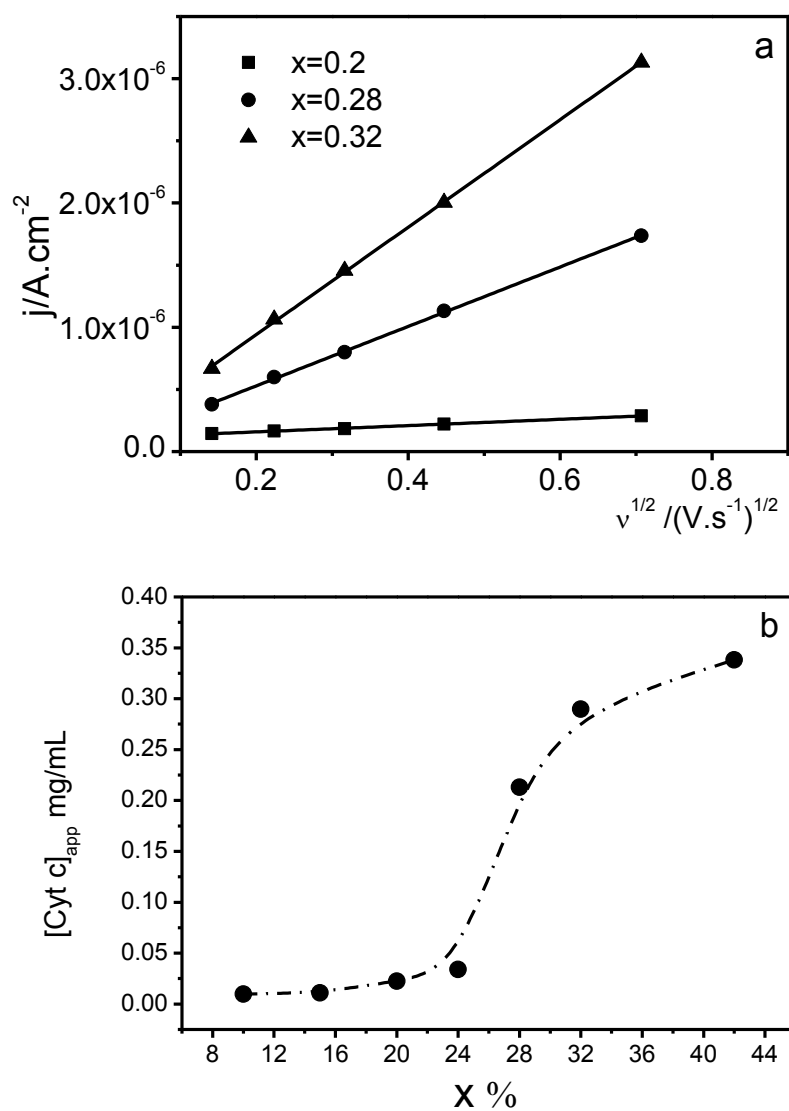
18

Figure 7. (a) Plot of anodic peak current versus the square root of the scan rate for cyt c@SiO$_{(2-0.5x)}$Me$_x$ modified electrodes in PBS. (b) Dependence of the encapsulated cyt c apparent concentration on the mole fraction of methyl groups present in the ormosil structure.

In any case, linear dependences of the peak current on the square root of the scan rate are found. Since this behavior implies a diffusion-controlled electrode process, it should be assumed that the electron transfer takes place from the electrode surface to cyt c molecules which retain part of their bulk free movement although they are encapsulated. Indeed, the silica hydrogel is often considered as a two-phase system consisting in a porous solid and a trapped aqueous phase [54]. We have found that the results obtained here contrast with those reported previously by Wang et al. for several hemoproteins, including cyt c, entrapped in agarose gel [55] for which, a linear dependence of the current with the scan rate was observed. Accordingly, it was suggested that the electron transfer could take place to hemoproteins fixed to the polysaccharide chains. Later, these results were revised by Lo Gorton [56] who pointed that heme groups fully, or partially, detached from the protein were responsible for the observed electrochemical reaction.

So, assuming that the immobilized cyt c stands in an encapsulating aqueous environment similar to the bulk solution, Randles-Sevcik equations can be used to obtain the apparent concentration of this biomolecule within the silica pore. Values of the apparent concentration are presented in Fig. 7.b as a function of the molar fraction of methyl groups in the silica. It can be observed that for silica gels containing up to 24% methyl groups, the apparent concentration of cyt c remains really low (less than 3μM, that is less than 8% of the encapsulated protein). However, when the methyl group content exceeds a threshold value of 24%, an abrupt increase in the apparent concentration of cyt c occurs and values as high as 20 μM are then obtained.

This behavior may be related with the structural characteristics of *ormosils*. It is thought that low levels of organosilanes in the precursor solution facilitate their homogeneous dispersion within the pores of the final material. This is because the triethoxymethylsilane precursor is preferentially located at the pore interface, as the

20

methyl group prevents the polymer chain growth at its position. This leads to a regular change in the polarity of the material as the amount of organosilane is increased. However, high triethoxymethylsilane levels may lead to phase segregation owing to the existence of a critical point for the self-association of the organic components. This yields an open porous structure showing little interactions with cyt c [29].

It has been observed that the amount of methyl groups has an effect on both the electrochemical reversibility of the redox process (Fig. 6) and the cyt c apparent concentration inside the silica material (Fig. 7). In other words, it appears a correlation between reversibility and concentration which has already been reported by other authors [37,55,57]. According to the literature, this behavior can be due to the affinity shown by cyt c to the surface of metal oxide electrodes [58]. At low apparent concentrations, the electrochemical behavior of cyt c corresponds to an ideal reversible system, whose peak separation approaches 59 mV, revealing fast electron transfer to the bare ITO surface. However, higher cyt c concentrations may favor the adsorption of a protein layer on the ITO surface which hinders the electron transfer process and, obviously, disturbs the reversibility of the electrochemical reaction.

Now, we will return to the question of the possible conformational changes induced in cyt c by the presence of methyl groups in the silica pores. To check this, further *in-situ* UV-visible experiments have been conducted for the cyt c@$SiO_{1.86}Met_{0.28}$ electrode in PBS electrolyte. The spectrum (a) in Fig. 8 was acquired at open circuit and shows clearly the characteristic features of ferricytochrome c: the Soret band located at 409 nm and the poorly resolved α and *β* bands that appear in the vicinity of 530 nm. Upon electrochemical reduction at 0.2V, the shape of the UV-vis spectra changes to the characteristic profile of reduced cytochrome. In this way, the Soret band shifts slightly to 410 nm, whereas α and β bands get resolved appearing at 549 nm and 520 nm,

respectively. Cyt c is retained inside the silica during the experiments as revealed by the stability of the cyclic voltammograms recorded during the time interval of the experiments, which was longer than 2 hours.
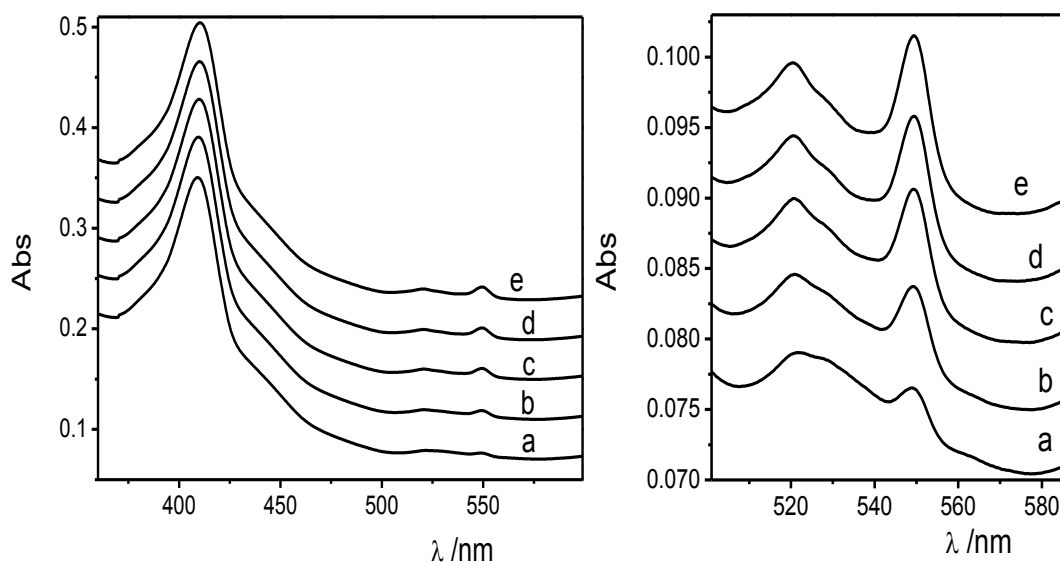

Figure 8. *In situ* UV-Vis spectra collected for a cyt c@SiO$_{1.86}$Met$_{0.28}$ modified electrode in PBS medium. Spectrum (a) was obtained first under open circuit conditions. After the application of a reduction potential of +0.2 V vs RHE, the following spectra were acquired at different times: 600 s (b), 1200s (c), 1600s (d) and 2000 s (e).

4. Conclusions

Cytochrome c encapsulated in different silica matrices was deposited on ITO electrodes. Cyt c@SiO$_2$ was synthesized via a two-step encapsulation method, mixing a

buffer solution with dissolved cytochrome c and a silica sol prepared by the alcohol free sol-gel route. These modified electrodes were characterized by cyclic voltammetry and UV-visible spectroscopy. Cyclic voltammetry indicates that the direct electron transfer between encapsulated cytochrome c and ITO electrodes takes place only for silica films where the methyl groups were incorporated, while conventional silica synthesized from pure TEOS or phenyl-modified silica do not show any electrochemical response. UV-visible spectroscopy experiments reveal negligible changes in the structural conformation of the encapsulated cytochrome c. The optical features of cytochrome c in silica were similar to cytochrome c in solution. From the experimental results presented in this paper it is expected that the electrochemical response of encapsulated proteins could be influenced by the terminal groups of the silica pores. These groups induce changes in both the polarity and the hydrophobicity of the micro-environment that surround the biomolecule.

5. Acknowledgements

References

1. Busalmen, J. P.; Esteve-Núñez, A.; Berná, A.; Feliu, J. M. C-Type Cytochromes Wire Electricity-Producing Bacteria to Electrodes. *Angewandte Chemie* **2008,** *120* (26), 4952-4955.

2. Schroder, U. Anodic electron transfer mechanisms in microbial fuel cells and their energy efficiency. *Phys. Chem. Chem. Phys.* **2007,** *9* (21), 2619-2629.

3. Rosenbaum, M.; Aulenta, F.; Villano, M.; Angenent, L. T. Cathodes as electron donors for microbial metabolism: Which extracellular electron transfer mechanisms are involved? *Bioresource Technology* **2011,** *102* (1), 324-333.

4. Jain, A.; Zhang, X.; Pastorella, G.; Connolly, J. O.; Barry, N.; Woolley, R.; Krishnamurthy, S.; Marsili, E. Electron transfer mechanism in Shewanella loihica PV-4 biofilms formed at graphite electrode. *Bioelectrochemistry* **2012,** *87* (0), 28-32.

5. Dodhia, V. R.; Sassone, C.; Fantuzzi, A.; Nardo, G. D.; Sadeghi, S. J.; Gilardi, G. Modulating the coupling efficiency of human cytochrome P450 CYP3A4 at electrode surfaces through protein engineering. *Electrochemistry Communications* **2008,** *10* (11), 1744-1747.

6. Renault, C.; Andrieux, C. P.; Tucker, R. T.; Brett, M. J.; Balland, V. +.; Limoges, B. t. Unraveling the Mechanism of Catalytic Reduction of O2 by Microperoxidase-11 Adsorbed within a Transparent 3D-Nanoporous ITO Film. *J. Am. Chem. Soc.* **2012,** *134* (15), 6834-6845.

7. Qian, W.; Sun, Y. L.; Wang, Y. H.; Zhuang, J. H.; Xie, Y.; Huang, Z. X. The Influence of Mutation at Glu44 and Glu56 of Cytochrome b_5 on the Protein's Stabilization and Interaction between Cytochrome c and Cytochrome b_5. *Biochemistry* **1998,** *37* (40), 14137-14150.

8. Cass, A. E. G.; Davis, G.; Francis, G. D.; Hill, H. A.; Aston, W. J.; Higgins, I. J.; Plotkin, E. V.; Scott, L. D. L.; Turner, A. P. F. Ferrocene-mediated enzyme electrode for amperometric determination of glucose. *Anal. Chem.* **1984,** *56* (4), 667-671.

9. Wang, B.; Li, B.; Deng, Q.; Dong, S. Amperometric Glucose Biosensor Based on Sol−Gel Organic−Inorganic Hybrid Material. *Anal. Chem.* **1998,** *70* (15), 3170-3174.

10. Kosela, E.; Elzanowska, H.; Kutner, W. Charge mediation by ruthenium poly(pyridine) complexes in 'second-generation' glucose biosensors based on carboxymethylated β−cyclodextrin polymer membranes. *Anal Bioanal Chem* **2002,** *373* (8), 724-734.

11. Guo, Z.; Chen, J.; Liu, H.; Cha, C. Direct electrochemistry of hemoglobin and myoglobin at didodecyldimethylammonium bromide-modified powder microelectrode and application for electrochemical detection of nitric oxide. *Analytica Chimica Acta* **2008,** *607* (1), 30-36.

12. Jia, J.; Wang, B.; Wu, A.; Cheng, G.; Li, Z.; Dong, S. A Method to Construct a Third-Generation Horseradish Peroxidase Biosensor: Self-Assembling Gold Nanoparticles to Three-Dimensional Sol−Gel Network. *Anal. Chem.* **2002,** *74* (9), 2217-2223.

13. Xu, J. S.; Zhao, G. C. Direct Electrochemistry of Cytochrome c on a Silica Sol-Gel Film Modified Electrode. *Electroanalysis* **2008,** *20* (11), 1200-1203.

14. Zhao, G. C.; Yin, Z. Z.; Zhang, L.; Wei, X. W. Direct electrochemistry of cytochrome c on a multi-walled carbon nanotubes modified electrode and its electrocatalytic activity for the reduction of H_2O_2. *Electrochemistry Communications* **2005,** *7* (3), 256-260.

15. Kafi, A. K. M.; Lee, D. Y.; Park, S. H.; Kwon, Y. S. Development of a peroxide biosensor made of a thiolated-viologen and hemoglobin-modified gold electrode. *Microchemical Journal* **2007,** *85* (2), 308-313.

16. Suárez, G.; Santschi, C.; Martin, O. J. F.; Slaveykova, V. I. Biosensor based on chemically-designed anchorable cytochrome c for the detection of H_2O_2 released by aquaticcells. *Biosensors and Bioelectronics* **2013,** *42* (0), 385-390.

17. Fu, C.; Yang, W.; Chen, X.; Evans, D. G. Direct electrochemistry of glucose oxidase on a graphite nanosheet−Nafion composite film modified electrode. *Electrochemistry Communications* **2009,** *11* (5), 997-1000.

18. Deng, S.; Jian, G.; Lei, J.; Hu, Z.; Ju, H. A glucose biosensor based on direct electrochemistry of glucose oxidase immobilized on nitrogen-doped carbon nanotubes. *Biosensors and Bioelectronics* **2009,** *25* (2), 373-377.

19. Stoica, L.; Ludwig, R.; Haltrich, D.; Gorton, L. Third-Generation Biosensor for Lactose Based on Newly Discovered Cellobiose Dehydrogenase. *Anal. Chem.* **2005,** *78* (2), 393-398.

20. Jin, B.; Wang, G. X.; Millo, D.; Hildebrandt, P.; Xia, X. H. Electric-Field Control of the pH-Dependent Redox Process of Cytochrome c Immobilized on a Gold Electrode. *J. Phys. Chem. C* **2012,** *116* (24), 13038-13044.

21. Koposova, E.; Kisner, A.; Shumilova, G.; Ermolenko, Y.; Offenh+ñusser, A.; Mourzina, Y. Oleylamine-Stabilized Gold Nanostructures for Bioelectronic Assembly. Direct Electrochemistry of Cytochrome c. *J. Phys. Chem. C* **2013,** *117* (27), 13944-13951.

22. Alegret, S.; Céspedes, F.; Martínez-Fábregas, E.; Martorell, D.; Morales, A.; Centelles, E.; Muñoz, J. Carbon-polymer biocomposites for amperometric sensing. *Biosensors and Bioelectronics* **1996,** *11* (1−2), 35-44.

23. Wang, Q.; Lu, G.; Yang, B. Myoglobin/Sol−Gel Film Modified Electrode:Direct Electrochemistry and Electrochemical Catalysis. *Langmuir* **2004,** *20* (4), 1342-1347.

24. Tripathi, V. S.; Kandimalla, V. B.; Ju, H. Preparation of ormosil and its applications in the immobilizing biomolecules. *Sensors and Actuators B: Chemical* **2006,** *114* (2), 1071-1082.

25. Jin, W.; Brennan, J. D. Properties and applications of proteins encapsulated within sol-gel derived materials. *Analytica Chimica Acta* **2002,** *461* (1), 1-36.

26. Gill, I.; Ballesteros, A. Encapsulation of Biologicals within Silicate, Siloxane, and Hybrid Sol-Gel Polymers: An Efficient and Generic Approach. *J. Am. Chem. Soc.* **1998,** *120* (34), 8587-8598.

27. Fried, D. I.; Brieler, F. J.; Fröba, M. Designing Inorganic Porous Materials for Enzyme Adsorption and Applications in Biocatalysis. *ChemCatChem* **2013,** *5* (4), 862-884.

28. Bhatia, R. B.; Brinker, C. J.; Gupta, A. K.; Singh, A. K. Aqueous Sol−Gel Process for Protein Encapsulation. *Chem. Mater.* **2000,** *12* (8), 2434-2441.

29. Keeling-Tucker, T.; Brennan, J. D. Fluorescent Probes as Reporters on the Local Structure and Dynamics in Sol-Gel-Derived Nanocomposite Materials. *Chem. Mater.* **2001,** *13* (10), 3331-3350.

30. Dunn, B.; Zink, J. I. Probes of Pore Environment and Molecule−Matrix Interactions in Sol−Gel Materials. *Chem. Mater.* **1997,** *9* (11), 2280-2291.

31. Murphy, M. P. How mitochondria produce reactive oxygen species. *Biochem J* **2009,** *417* (1), 1-13.

32. Green, D. R.; Reed, J. C. Mitochondria and apoptosis. *Science-AAAS-Weekly Paper Edition* **1998,** *281* (5381), 1309-1311.

33. Ghach, W.; Etienne, M.; Urbanova, V.; Jorand, F. P. A.; Walcarius, A. Sol−gel based 'artificial' biofilm from Pseudomonas fluorescens using bovine heart cytochrome c as electron mediator. *Electrochemistry Communications* **2014,** *38* (0), 71-74.

34. Gamero-Quijano, A.; Huerta, F.; Salinas-Torres, D.; Morallón, E.; Montilla, F. Enhancement of the Electrochemical Performance of SWCNT dispersed in a Silica Sol-gel Matrix by Reactive Insertion of a Conducting Polymer. *Electrochimica Acta* **2014,** *135* (0), 114-120.

35. Collinson, M.; Bowden, E. F. UV-visible spectroscopy of adsorbed cytochrome c on tin oxide electrodes. *Anal. Chem.* **1992,** *64* (13), 1470-1476.

36. Eddowes, M. J.; Hill, H. A. Electrochemistry of horse heart cytochrome c. *J. Am. Chem. Soc.* **1979,** *101* (16), 4461-4464.

37. Bowden, E. F.; Hawkridge, F. M.; Chlebowski, J. F.; Bancroft, E. E.; Thorpe, C.; Blount, H. N. Cyclic voltammetry and derivative cyclic voltabsorptometry of purified horse heart cytochrome c at tin-doped indium oxide optically transparent electrodes. *J. Am. Chem. Soc.* **1982,** *104* (26), 7641-7644.

38. Hawkridge, F.; Kuwana, T. Indirect coulometric titration of biological electron transport components. *Anal. Chem.* **1973,** *45* (7), 1021-1027.

39. Armstrong, F. A.; Hill, H. A.; Oliver, B. N. Surface selectivity in the direct electrochemistry of redox proteins. Contrasting behaviour at edge and basal planes of graphite. *Journal of the Chemical Society, Chemical Communications* **1984,** (15), 976-977.

40. El Kasmi, A.; Leopold, M. C.; Galligan, R.; Robertson, R. T.; Saavedra, S. S.; El Kacemi, K.; Bowden, E. F. Adsorptive immobilization of cytochrome c on indium/tin oxide (ITO): electrochemical evidence for electron transfer-induced conformational changes. *Electrochemistry Communications* **2002,** *4* (2), 177-181.

41. Gamero-Quijano, A.; Huerta, F.; Salinas-Torres, D.; Morallón, E.; Montilla, F. Electrochemical Behaviour of PSS-Functionalized Silica Films Prepared by Electroassisted Deposition of Sol−Gel Precursors. *Electrocatalysis* **2014,** *in press* DOI 10.1007/s12678-014-0215-0.

42. Haymond, S.; Babcock, G. T.; Swain, G. M. Direct Electrochemistry of Cytochrome c at Nanocrystalline Boron-Doped Diamond. *J. Am. Chem. Soc.* **2002,** *124* (36), 10634-10635.

43. Collinson, M. M.; Howells, A. R. Peer Reviewed: Sol−Gels and Electrochemistry: Research at the Intersection. *Anal. Chem.* **2000,** *72* (21), 702-709.

44. Washmon-Kriel, L.; Jimenez, V. L.; Balkus, J. Cytochrome c immobilization into mesoporous molecular sieves. *Journal of Molecular Catalysis B: Enzymatic* **2000,** *10* (5), 453-469.

45. Lan, H.; Dave, C.; Fukuto, M.; Dunn, B.; Zink, I.; Valentine, S. Synthesis of sol-gel encapsulated heme proteins with chemical sensing properties. *J. Mater. Chem.* **1999,** *9* (1), 45-53.

46. Dave, B. C.; Soyez, H.; Miller, J. M.; Dunn, B.; Valentine, J. S.; Zink, J. I. Synthesis of Protein-Doped Sol-Gel SiO_2 Thin Films: Evidence for Rotational Mobility of Encapsulated Cytochrome c. *Chem. Mater.* **1995,** *7* (8), 1431-1434.

47. Flora, K.; Brennan, J. D. Fluorometric Detection of Ca^{2+} Based on an Induced Change in the Conformation of Sol−Gel Entrapped Parvalbumin. *Anal. Chem.* **1998,** *70* (21), 4505-4513.

48. Vinu, A.; Murugesan, V.; Tangermann, O.; Hartmann, M. Adsorption of Cytochrome c on Mesoporous Molecular Sieves: Influence of pH, Pore Diameter, and Aluminum Incorporation. *Chem. Mater.* **2004,** *16* (16), 3056-3065.

49. Brinker, C. F. S. G. W. *Sol-Gel Science: The Physics and Chemistry of Sol-Gel Prcessing;* Academid Press Limited: San Diego, CA 92101, 1990.

50. J.P.Brunelle Preparation of catalysts by metallic complex adsorption on mineral oxides. *Pure Appl. Chem.* **1978,** *50* (9-10), 1211-1229.

51. Keeling-Tucker, T.; Rakic, M.; Spong, C.; Brennan, J. D. Controlling the Material Properties and Biological Activity of Lipase within Sol−Gel Derived Bioglasses via Organosilane and Polymer Doping. *Chem. Mater.* **2000,** *12* (12), 3695-3704.

52. Wen, J.; Wilkes, G. L. Organic/Inorganic Hybrid Network Materials by the Sol−Gel Approach. *Chem. Mater.* **1996,** *8* (8), 1667-1681.

53. Nadzhafova, O.; Etienne, M.; Walcarius, A. Direct electrochemistry of hemoglobin and glucose oxidase in electrodeposited sol−gel silica thin films on glassy carbon. *Electrochemistry Communications* **2007,** *9* (5), 1189-1195.

54. Shen, C.; Kostic´, N. M. Kinetics of Photoinduced Electron-Transfer Reactions within Sol-Gel Silica Glass Doped with Zinc Cytochrome c. Study of Electrostatic Effects in Confined Liquids. *J. Am. Chem. Soc.* **1997,** *119* (6), 1304-1312.

55. Wang, S. F.; Chen, T.; Zhang, Z. L.; Shen, X. C.; Lu, Z. X.; Pang, D. W.; Wong, K. Y. Direct Electrochemistry and Electrocatalysis of Heme Proteins Entrapped in Agarose Hydrogel Films in Room-Temperature Ionic Liquids. *Langmuir* **2005,** *21* (20), 9260-9266.

56. Brusova, Z.; Gorton, L.; Magner, E. Comment on direct electrochemistry and electrocatalysis of heme proteins entrapped in agarose hydrogel films in room-temperature ionic liquids. *Langmuir* **2006,** *22* (26), 11453-11455.

57. Yoshioka, K.; Kato, D.; Kamata, T.; Niwa, O. Cytochrome P450 Modified Polycrystalline Indium Tin Oxide Film as a Drug Metabolizing Electrochemical Biosensor with a Simple Configuration. *Anal. Chem.* **2013,** *85* (21), 9996-9999.

58. McKenzie, K. J.; Marken, F. Accumulation and Reactivity of the Redox Protein Cytochrome c in Mesoporous Films of TiO_2 Phytate. *Langmuir* **2003,** *19* (10), 4327-4331.